ADVANCED MATERIALS INTERFACES

www.advmatinterfaces.de

Enhancement of Wetting and Mechanical Properties of UHMWPE-Based Composites through Alumina Atomic Layer Deposition

*Meni Shimel, Irina Gouzman, Eitan Grossman, Zahava Barkay, Sari Katz, Asaf Bolker, Noam Eliaz, and Ronen Verker**

Ultrahigh molecular weight polyethylene (UHMWPE) fibers suffer from poor adhesion to polar matrices in composites due to their chemically inert surface, thus limiting the use of UHMWPE-based fabrics and composites. Atomic layer deposition (ALD) is a useful method of constructing a thin oxide layer, with a variety of oxides available, enabling a nondestructive method for surface modification. Here, UHMWPE fibers and fabrics are coated by ALD with a thin alumina layer, using two precursors—trimethylaluminum (TMA) and water—to a final coating thickness of 39 nm. The effect of the oxide coating layer is determined by various mechanical and physical tests. The contact angle is reduced by 44–49%, indicating a substantial increase in wettability. Significant improvements are observed in the flexural modulus, flexural strength, interlaminar shear strength, resilience, and toughness. Frequency dependence tests show an improvement in storage modulus at all tested frequencies, insinuating higher impact toughness at high strain rates. Failure analysis reveals a change in the failure mode, from pinholes formation and adhesion failure to cohesion failure and mixed failure modes. Thus, the use of ALD alumina-coated UHMWPE fibers in composites shows high scientific and technological potential.

1. Introduction

Ultrahigh molecular weight polyethylene (UHMWPE) fibers gained popularity during the late 1980s due to their superior mechanical properties compared to nylon and Kevlar fibers, which were predominant at that time.[1–3] Its current industrial applications are mainly as a textile material for ropes, cables, and wires.[4–6] Its defense applications include ballistic protection, e.g., bullet-proof vests and helmets, and applications where low friction, specific strength, and exposure to harsh conditions are required. For example, in marine applications where there is constant exposure to outdoor environment and UV radiation.[7] Theoretically, UHMWPE fibers are an excellent choice as a reinforcing fiber material in composite materials due to their outstanding mechanical properties, e.g., high modulus and impact resistance, and high chemical resistance.[8] Unfortunately, UHMWPE suffers from a few limitations. One of these is its fairly narrow temperature range of operation: its melting range starts at 144 °C, but already at 70 °C its mechanical properties start to degrade, and creep already begins at ambient temperatures.[6,9,10] In addition, and perhaps even more important, the reason for the lack of adoption of UHMWPE as a reinforcing material in composites is its chemical inertness, which results in poor wettability of polar and/or hydrophilic matrices, such as epoxy and polyester.[11–15] The poor wettability of UHMWPE results in low interfacial bond strength compared to other synthetic reinforcing agents, such as aramid fibers.[12,16,17] Thus, surface modification of the UHMWPE fibers can help in overcoming two inherent disadvantages—poor wettability and poor intrafibrillar connectivity.[6,10]

Traditionally, efforts to improve wettability or adhesion in composites concentrate on treating either the reinforcer or the matrix. Matrix modification techniques aim to incorporate additives that affect the fiber/matrix interface and the wetting behavior. This approach is beneficial as the reinforcing fiber structure and mechanical properties are unaffected compared to fiber radiation-based (UV, gamma, etc.) processes. Several sets of additives have been added to resin systems in order to affect the resin/reinforcer wetting behavior, among them are graphitic nanofibers,[18] elastomer-based additives,[19] and carbon nanotubes (CNTs).[20]

M. Shimel, Dr. I. Gouzman, Dr. E. Grossman, Dr. S. Katz, Dr. A. Bolker, Dr. R. Verker
Space Environment Department
Soreq NRC
Yavne 81800, Israel
E-mail: rverker@soreq.gov.il
M. Shimel, Prof. N. Eliaz
Department of Materials Science and Engineering
Tel-Aviv University
Ramat Aviv, Tel-Aviv 6997801, Israel
Dr. Z. Barkay
Wolfson Applied Materials Research Center
Tel-Aviv University
Ramat Aviv, Tel-Aviv 6997801, Israel
The ORCID identification number(s) for the author(s) of this article can be found under https://doi.org/10.1002/admi.201800295.

DOI: 10.1002/admi.201800295

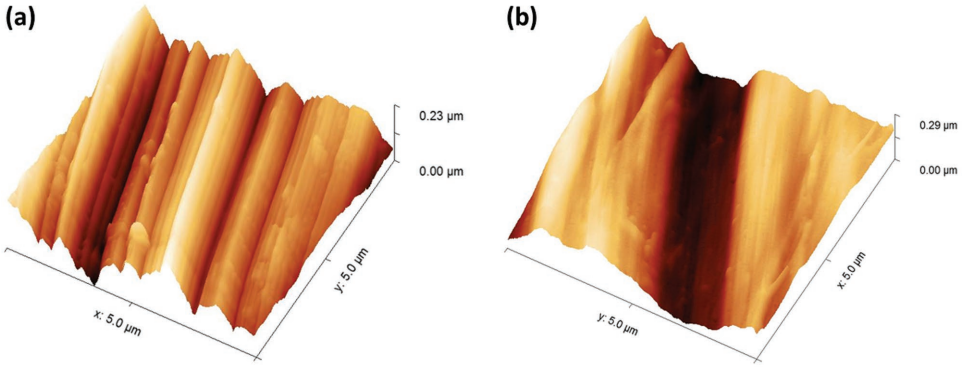

Figure 1. AFM images of fiber surface morphology of a) pristine fabric and b) alumina-coated fabric.

A plethora of different techniques was implemented to modify the fiber's surface. Pyrrole coating has shown a large increase in adhesion to polar matrices by increasing drastically the surface roughness and surface energy of UHMWPE fibers.[21,22] Fluorination on the surface led to surface roughening and improvement in adhesion strength.[23] Further chemical surface modifications included UV radiation-grafting of acrylate-based polymers[24] and silane-based groups,[25,26] all used surface roughening for adhesion improvement. Plasma etching[13,17,27–29] and radiation techniques such as UV or electron-beam irradiation[25,26] were implemented to produce surface roughening to achieve superior bonding strength, similarly to previous methods. However, high-energy oncoming beam has a high penetration depth, causing chain scission reactions, and thereby reduction of the fiber integrity and its overall mechanical properties.[13,24,28] Moreover, plasma methods have a time-sensitive beneficial effect, as polymers regenerate, and surface activation is not stable. Most of these previous studies were performed on single UHMWPE fiber threads. The bonding strength was measured by pull-out tests (or a parallel method), or by incorporating small chopped treated fibers in a matrix. However, in most of these previous works, the effect of the coating on the fiber's mechanical properties was not reported.

Surface modification by oxide layer deposition is very common in many applications, ranging from microelectronics to passivation layers and gas permeation barriers. Atomic layer deposition (ALD), which was developed during the 1980s, has emerged as a thin-layer oxide deposition process and as a subclass of chemical vapor deposition (CVD) techniques.[30] In recent years, this method has been applied on polymer substrates such as polypropylene (PP), polymethylmethacrylate (PMMA), and polyethylene (PE).[30–32] Thus, it has ignited research on different substrates for ALD deposition, such as fibrous materials. The ability for oxide layer formation on polymeric fiber substrates without the need to use harsh chemicals or processes, such as long plasma etching, is a promising technique to enhance adhesion without degrading the mechanical properties. Previous studies investigated the alumina (Al_2O_3) layer formation on single fiber threads of UHMWPE for adhesion promotion.[33] This led us to study the interface characteristics of an alumina nanometric layer as a nondestructive adhesion promoter for UHMWPE fabrics to polar matrices, such as epoxy, for the construction of novel composite laminate materials with enhanced mechanical properties. The significance of this study is the performance of surface modification on a large-scale 3D structure (fabric), in contrast to previous works that investigated 1D single fibers or flat 2D polymer films. Moreover, the fabrics were used in a laminate structure, similarly to what an end-user will use, thus evaluating the contribution of the ALD alumina coating process to the enhancement of mechanical properties of a case-study composite laminate with a potential to be used in near-future applications.

2. Results and Discussion

2.1. Fiber Surface Characterization

Representative AFM images revealing the surface morphology of pristine and alumina-coated fibers are shown in **Figure 1**. Figure 1a shows the microfibrillar structure of the pristine UHMWPE fibers, which is in agreement with results reported by others.[34–36] Figure 1b shows the fiber morphology after alumina coating. Examination of the surface of the fibers before and after alumina layer deposition leads to the conclusion that the oxide layer conforms to the surface of the fibers, without any formation of cracks.

Surface roughness line scan data, which are presented in Table S1 in the Supporting Information, show that the roughness average (R_a) of the alumina-coated fibers is slightly lower compared to the roughness of the pristine fibers (3.3 and 5.6 nm, respectively). These results imply that the coating is semiconformal[30,37–39] and provides some "smoothing" effect, which may be related to the oxide layer formation. The oxide surface species (AlOH*) are formed as clusters or islands, which coalesce to form a uniform layer after sufficient cycles have been completed. Beyond that point, the surface roughness is normally similar to the underlying surface.[37,39,40] When the surface roughness of the fibers is of the same magnitude as the coating thickness, filling of valleys can explain the smoothing observed.

Comparably, inspecting the UHMWPE fiber surface by scanning electron microscopy (SEM) does not reveal any significant macroscopic changes in the surface morphology after the ALD

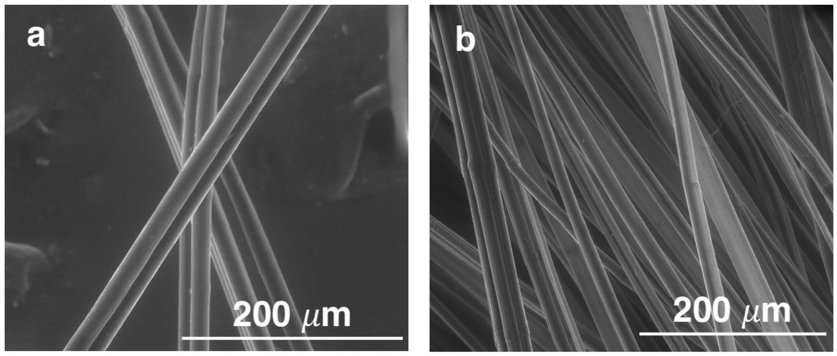

Figure 2. SEM images of a) pristine and b) alumina-coated UHMWPE fibers.

treatment, as seen in **Figure 2**. Some impurities are visible on the coated fibers; however, the surfaces seem similar before and after the ALD coating process.

Energy dispersive X-ray spectroscopy (EDS) analysis was performed in order to study the presence and uniformity of the alumina coating on the fiber surface (**Figure 3**). The fabric for this analysis was unstitched in order to expose fibers far below the fabric's surface, thus allowing assessment of the efficiency of the ALD technique in coating the fibers at regions relatively hard to reach by the precursors. Figure 3a shows the SEM image of the fibers on which the EDS analysis was performed. Figure 3b–d shows the carbon, aluminum, and oxygen atomic mapping, respectively. The EDS analysis shows the ability of the ALD technique to allow penetration of the precursors deep into the UHMWPE fabric and to form the alumina coating on fibers far below its surface.

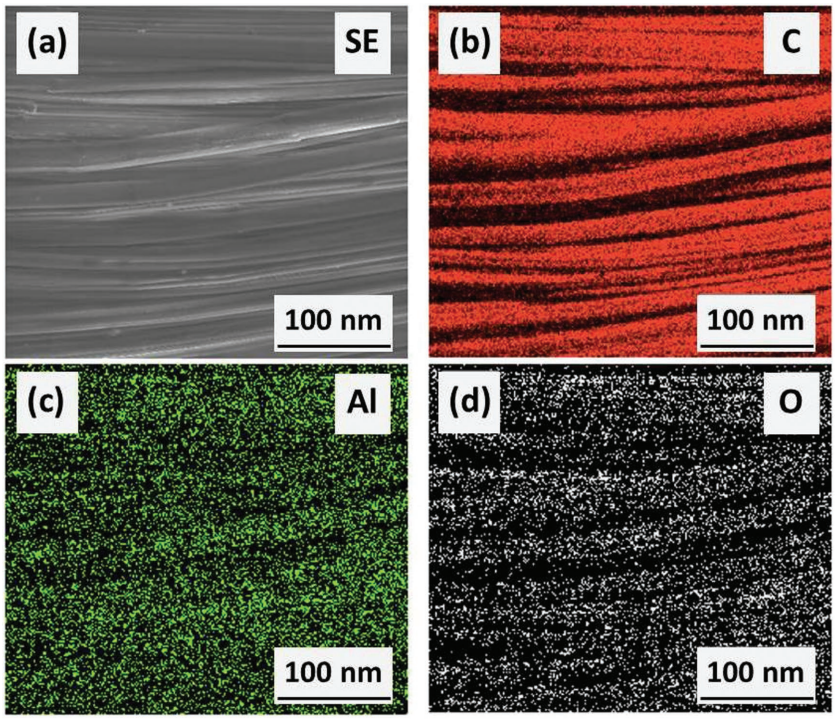

Figure 3. EDS elemental mapping of alumina-coated UHMWPE fibers. a) Image shows the SE image of the area on which EDS analysis was performed. b–d) Images show the carbon, aluminum, and oxygen element mapping, respectively.

2.2. In Situ Contact Angle Measurement by ESEM

Wettability study of surfaces at high spatial resolution is an emerging field in smooth and textured materials characterization.[41–43] By elevating the environmental scanning electron microscope (ESEM) conditions above dew point, micron-scale water droplets condense on the sample surface, enabling the study of contact angle on small sample geometries comparable to droplet size. In several studies[41,44] it was shown that in comparison to other methods, the contact angle measurement by the ESEM condensation method provides a reliable measurement method. In this study, the fiber average typical diameter was ≈20 μm. Therefore, the study referred to in situ imaging of micron-size droplet condensation. The measured angles referred to side-view images of drops in the initial condensation stage. Large droplets were omitted from the analysis as they do not represent the first stage of wetting. A contact angle comparison was performed between single threads taken from fibers and from the fabric of UHMWPE, before and after alumina coating. It provided estimation of the efficiency of coating on a complex structure such as the fabric. In the case of fabric samples, a small section of the fabric was cut and spread across a sample holder in order to investigate fibers that were situated at both the outer and inner layers of the fabric. Typical images are presented in **Figure 4**, comparing droplets deposited on UHMWPE threads taken from fibers to those taken from fabric. Summary of the contact angle data is presented in **Table 1**. The error of measurement represents one standard deviation. Epoxy resins have a range of surface tensions that are determined by the monomers chosen. Where low viscosity resins are used, such as in our case, it was found that the surface tension is fairly close to that of water.[45] Taking into account the presence of hydrogen bonds both in water and in the epoxy resin, we can assume that the water contact angle reduction we found should predict qualitatively a similar behavior when low-viscosity epoxy resin is used in contact with the alumina coating compared with the pristine UHMWPE surface.

The alumina layer deposited by ALD reduces the contact angle on threads taken from fiber and fabric by 44% and 49%, respectively. Despite the close packing of the fabric, the ALD of alumina coating on fabrics is as efficient as that on fibers. In the case of pristine UHMWPE, the different contact angles on threads taken from commercial fibers and threads taken from

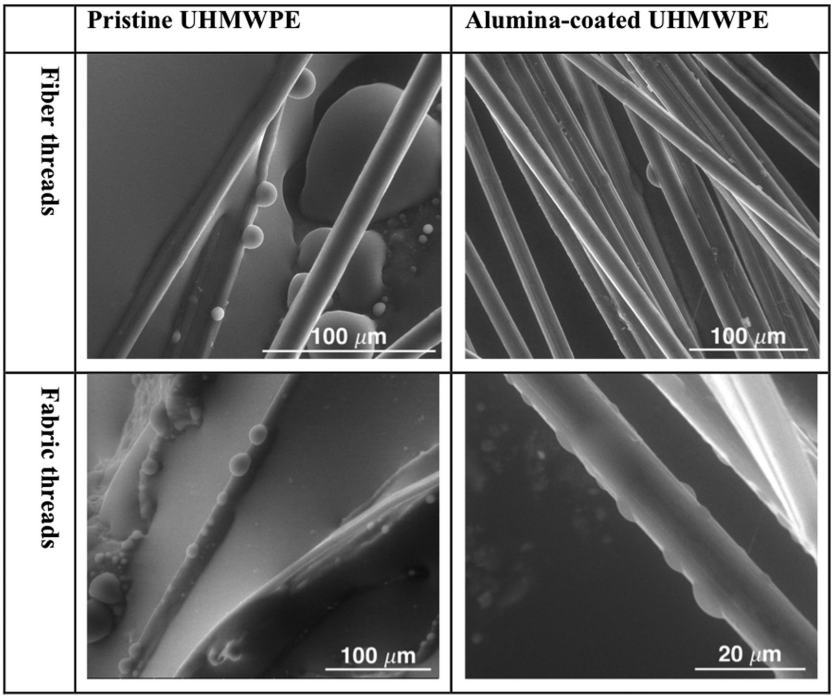

Figure 4. Comparison between the contact angle of water droplets on pristine and alumina-coated threads taken from fiber and fabric surfaces.

commercial fabric may result from different fabrication processes performed on the fiber strand. In the case of the commercial fiber, a sizing coating was applied to reduce fiber fusion during winding. The sizing had been removed before contact angle measurements were performed. In contrast, the threads from the fabric were not coated with any sizing, but were corona treated instead. The corona treatment is usually done when better adhesion is required, as reflected by the lower contact angle. The alumina coating on the fabric samples is thicker than that on the fibers. The reason for this is the longer diffusion time between purges in order to facilitate reagent absorbance throughout the fabric, thus increasing the measured oxide layer thickness by 5 nm. The thickness of the oxide film has a "dose-response" effect on the reduction of the measured contact angle. This suggests that thicker layers may reduce it further. The above results demonstrate the ability of the reagents to penetrate the fibers within the fabric during the ALD process and to substantially increase the UHMWPE wettability.

Table 1. Contact angle measurements.

	Threads taken from fiber	Threads taken from fabric
Contact angle – pristine UHMWPE [°]	90.0 ± 5.1	74.6 ± 6.8
Contact angle – alumina coated UHMWPE [°]	50.6 ± 5.3	38.1 ± 6.5
Coating thickness [nm]	34 ± 4	39 ± 4
Percentage of contact angle decrease [%]	44%	49%

2.3. Fibers' Mechanical Properties

As mentioned, surface modification by ALD enables the formation of a conformal deposition of a nanometer-scale oxide layer. Another important aspect of surface modification of fibers is the potential negative effect on their mechanical properties, as described by others.[14,15,24,29,46] In order to determine whether the mechanical properties of the fibers were degraded as a result of the ALD process, individual fibers of UHMWPE were subjected to tensile tests via dynamic mechanical analysis (DMA). Ten samples of pristine and alumina-coated fiber samples, with diameters within the range of 16–28 μm, were tested. **Figure 5** shows the values of Young's modulus, tensile strength, and strain versus fiber diameter. Figure S3 (Supporting Information) shows the stress–strain behavior of pristine and alumina-coated fibers where these values are taken from. It is evident that fibers with smaller diameter exhibit better mechanical properties, both in the pristine and in the alumina-coated forms. This behavior, as well as the distribution of values, may be associated with a different linear density of the fibers, due to difference in the number of fibrils per fiber. Nevertheless, looking at the trend of tensile strength and Young's modulus in relation to fiber diameter—both populations show a similar behavior. However, strain values have decreased from 6.9 ± 1.5 in pristine fibers to 5.5 ± 0.7 in alumina-coated fibers, which is not a significant change. This leads to the conclusion that the alumina coating did not degrade the mechanical properties of the fibers in a significant way. This important advantage of ALD should be noted when aiming for influencing the surface without compromising fiber integrity.

2.4. Three-Point Bending Tests of UHMWPE-Epoxy Composites

The interlaminar shear strength (ILSS), flexural modulus, flexural strength, toughness, and resilience of pristine and alumina-coated UHMWPE-based composites were measured using the three-point bending technique. **Figure 6** shows stress–strain curves of composite laminates made from pristine and alumina-coated UHMWPE fabrics and epoxy matrix, tested by a Lloyd tensiometer with a three-point bending setup. The stress–strain curves in Figure 6 show two distinct clusters of data, one belongs to the pristine UHMWPE composite samples and the other to the alumina-coated UHMWPE-based composite. The mechanical properties were significantly improved, with no reduction in the overall elongation due to fracture, as a result of improved fiber/matrix adhesion. It has been reported that as the contact angle of the resin-on-fiber is decreased, load transfer is increased dramatically, as evident by mechanical properties enhancement.[13,15,22,29,47–49]

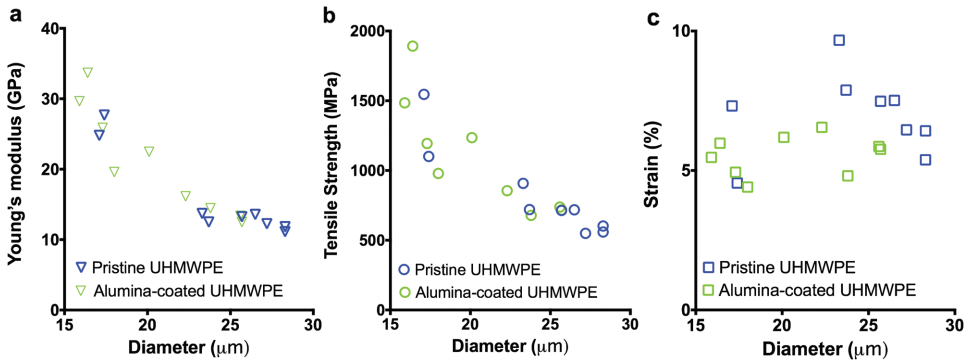

Figure 5. a) Young's modulus, b) tensile strength, and c) strain versus fiber diameter of the tested fibers. Tensile tests by DMA.

Figure 7 shows a graphical comparison that summarizes the measured mechanical properties. All results were found statistically significant according to Student's *t*-test ($p < 0.0001$). As shown in Figure 7, statistically significant property enhancement is found for all major parameters. For example, the ILSS and flexural strength were improved by 42% and 50%, respectively. The flexural modulus, resilience, and toughness increased by 38%, 46%, and 53%, respectively. These results emphasize the potential improvement of the mechanical properties of UHMWPE-based composites thanks to ALD alumina coating. The mechanical properties can be further enhanced by optimization of the coating thickness.

2.5. Frequency Sweep of UHMWPE-Epoxy Composites

DMA was utilized to characterize the mechanical response of the composite laminate to three-point bending at varying frequencies. This type of study implies the viscoelastic properties of the material, specifically its damping behavior which can be correlated with impact strength.[50,51] All tests were performed isothermally at 35 °C. The frequency sweep range was 0.05–200 Hz. **Figure 8** shows the frequency-dependence of a) the storage modulus, b) loss modulus, and c) tan delta.

The storage modulus versus frequency (Figure 8a) of the alumina-coated UHMWPE fabric-based composite shows the same behavior as the pristine fabric-based composite. However, the values of the former are higher, exemplifying the contribution of the ALD process to the improvement of the mechanical properties over a range of frequencies and, thus, strain rates. These results are in agreement with the three-point bending results shown earlier. In both types of composites, pristine and alumina-coated, the storage modulus increases as the frequency increases. The values of the loss modulus and tan delta show a decrease up to a frequency of 10 Hz, followed by an increase up to 200 Hz. The lower tan delta values of the composite samples made of alumina-coated fibers is an indication of the higher elasticity of these samples as a result of the ALD process. In general, during the frequency test, a material passes several stages: 1) The terminal zone, where the period of oscillation is so long that the polymer chains can snake through entanglement and rearrange their conformations. 2) The plateau zone, where the strain is accommodated by entropic changes to polymer segments between entanglements, providing good elastic response.[52] 3) The transition zone, where the period of oscillation is becoming too short to allow for complete rearrangement of chain conformation, and enough mobility is present for substantial friction between chain segments.[52] 4) The glassy zone, where no configurational rearrangements occur within the period of oscillation, stress response to a given strain is high (glass-like solid).

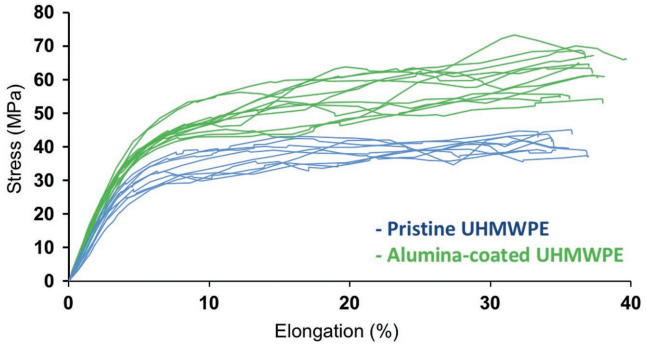

Figure 6. Stress–strain curves of the composite laminates made from pristine and alumina-coated UHMWPE fabrics and epoxy matrix.

In our case, the lower frequencies of 0.5–10 Hz were not low enough to represent the terminal zone. The lower frequencies represent the rubbery plateau zone, while the intermediate frequencies of 10–100 Hz represent the transition zone.[52] The highest frequencies of 100–200 Hz insinuate on the glassy region in the case of pristine UHMWPE fabric-based composite, and on a shift in the glassy zone of the alumina-coated UHMWPE fabric-based composite to higher frequencies, as seen in Figure 8b,c. Thus, an increase in impact energy at high frequencies is suggested. Since UHMWPE is considered as a ballistic defense material,[53,54] this result should trigger further study. These results coincide nicely with the increase in toughness and resilience that was previously shown based on three-point bending measurements.

2.6. Failure Analysis

In order to better understand the origin of the differences that were discovered by mechanical testing, the surfaces of three-point bended samples were characterized by high-resolution scanning electron microscope (HRSEM). Each sample was fully

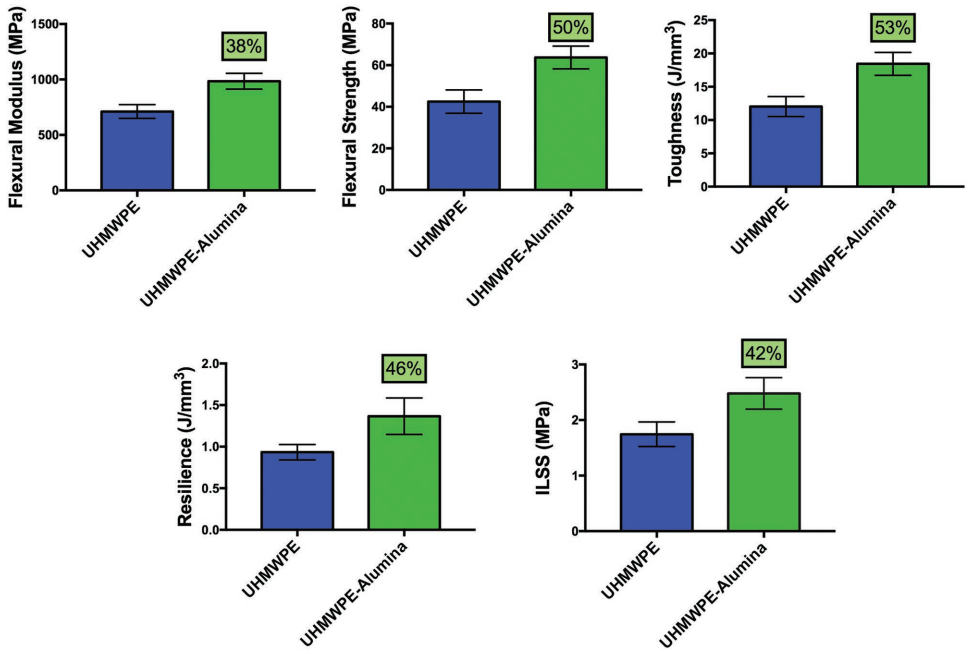

Figure 7. Mechanical properties based on three-point bending tests of pristine and alumina-coated UHMWPE-based composites.

bended and both edges were taped together, allowing for the study of the top convex area. In all samples, the air-side of the composite was studied, as shown in **Figure 9**.

Pinholes were found on the surface of pristine UHMWPE fabric-epoxy composite (Figure 9a). These pinholes are not visible in the case of alumina-coated UHMWPE fabric-epoxy composite (Figure 9b). This behavior can be explained by the poor wetting of epoxy on the pristine UHMWPE fabric, which causes the epoxy adhesive to reduce its contact surface with the fabric and, as a result, to generate voids at the UHMWPE/epoxy interface. This phenomenon can also be explained as poor adhesion, as suggested by others.[55–57] Furthermore, higher-magnification images reveal delamination between the pristine UHMWPE fibers and the epoxy matrix, seen in Figure 9c, where whole sections of epoxy layers were delaminated from the pristine fabric surface and voids are visible around the fibers (marked by a white arrow). These findings further support the theory of poor adhesion. In comparison, the alumina-coated UHMWPE fabric-epoxy laminate shows better adhesion, as a better epoxy-fiber wetting is seen in Figure 9d. It can be seen in this figure that a pulled-out fiber is still covered with an epoxy layer, and that a better cover of the epoxy layer exists (marked by white arrows).

2.7. Phenomenological Model

The addition of the alumina layer onto the UHMWPE fiber surface allows for water contact angle reduction by 44–49%, as found by in situ ESEM measurements. It also allows for better spreading of the epoxy around the UHMWPE fibers and better adhesion, as seen by the lack of pinholes at the alumina-coated UHMWPE-epoxy interface, compared to pristine fabric. The poor wetting between the pristine UHMWPE fabric and the epoxy resin results in the formation of these pinholes, which reduce the contact surface between the epoxy and the fibers. These pinholes contribute to the inferior mechanical properties compared to alumina-coated fabric, as they act as defects where

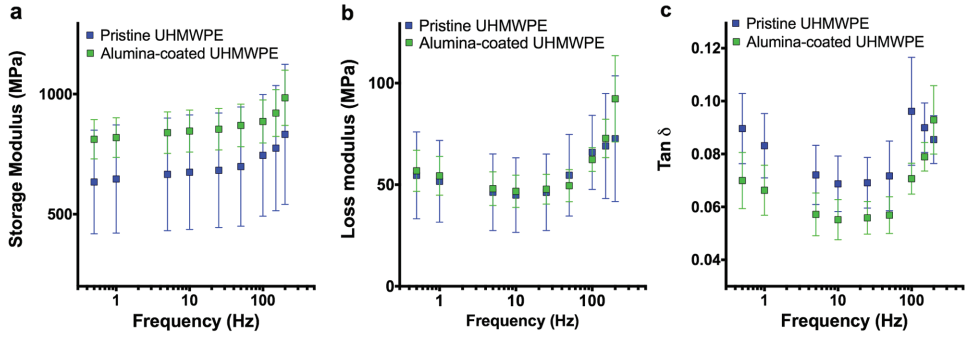

Figure 8. a) Storage modulus, b) loss modulus, and c) Tan delta of UHMWPE-epoxy laminates obtained from DMA frequency scans.

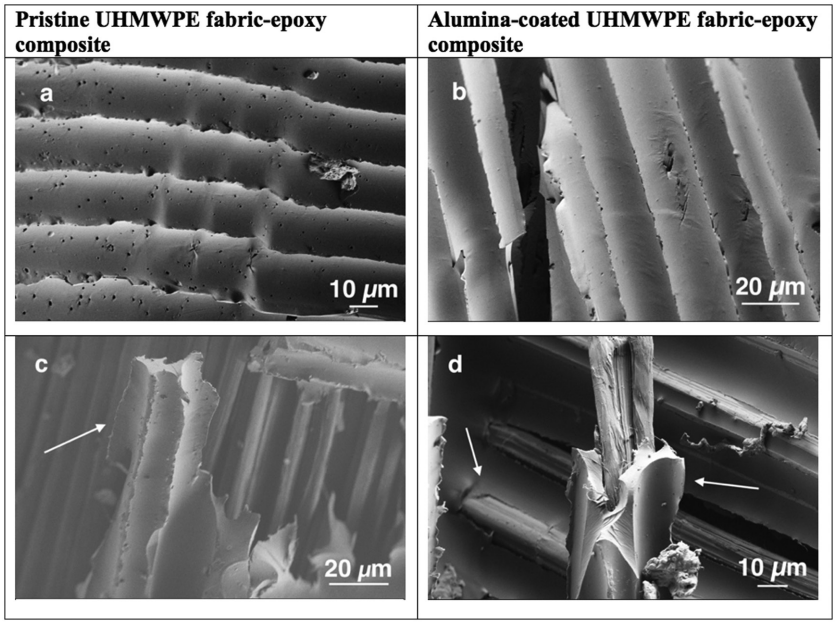

Figure 9. HRSEM images of a,c) fractured pristine and b,d) alumina-coated UHMWPE-epoxy composites.

failure can be initiated. As a result, the failure mechanism shifts from pinholes formation and adhesion failure in the case of pristine UHMWPE-base composite, to cohesion failure and mixed failure modes in the case of alumina-coated UHMWPE-based composite. The shift in failure mechanism of the laminates supports our previous results of adhesion and mechanical properties improvement.

3. Conclusion

Alumina-coated UHMWPE fabric–epoxy composites were prepared in order to investigate the viability of ALD as a method for surface modification of UHMWPE fabrics, aiming toward enhanced matrix-reinforcer fabric wetting and mechanical properties. This approach was chosen after previous single-fiber studies,[33] which do not fully correlate the behavior of laminate composites' structures, were performed. The ALD process has shown its viability as a nondestructive surface modification method for UHMWPE fibers. It was found that the alumina layer did not degrade the mechanical properties of the fibers, as often reported for other processes. EDS measurements showed that penetration of the alumina precursors species occurs throughout the fabric, thus further demonstrating the efficiency of the ALD process. A 44–49% decrease in contact angle of alumina-coated fibers compared to pristine fibers led to better fiber-matrix bond and, thus, to improved mechanical properties of the alumina-coated UHMWPE fabric-based composite laminates.

The lack of pinholes in alumina-coated UHMWPE-epoxy laminates, which allows for improved load transfer from fiber to matrix, and the change in failure mechanism further corroborate our findings. Mechanical properties evaluation showed a significant increase in major properties, such as flexural modulus, ILSS, flexural strength, resilience, and toughness. Furthermore, the shift of the glassy zone to higher frequencies, as measured by DMA, suggests an increase in impact strength in the alumina-coated UHMWPE fabric-based composite laminate.

Future research will entail identification of the optimal oxide layer thickness. We have shown that by increasing the alumina layer thickness from 34 to 39 nm, the contact angle reduction increases by 25% hinting at accumulative benefit.

In summary, the deposition of the alumina coating led to a significant improvement in UHMWPE-epoxy composite physical and mechanical properties. The long-term surface modification stability of the ALD alumina layer was shown as well. Hence, coating UHMWPE with a nanometric alumina layer, using the ALD technique, has great potential for future use in a wide range of applications involving UHMWPE.

4. Experimental Section

Materials: SK-75 Dyneema UHMWPE fibers were purchased from DSM, Netherlands. The sizing coating was removed prior to use (details are given in Section S1 in the Supporting Information). Plain weave UHMWPE fabric, with 8 warp and 6 weft threads cm^{-1}, based on SK-75 fibers, was purchased from Swiss-Composite, Switzerland. The fiber density was 0.97 g cm^{-3}, and the thickness of each fabric layer was 0.37 mm. The fabric was corona treated with no sizing coating and was used as-received for composite preparation. Araldite LY-5052 epoxy resin and Aradur 5052 epoxy hardener were purchased from Huntsman.[56] Trimethylaluminum ($Al(CH_3)_3$) from Sigma-Aldrich and 18 MΩcm water were used as precursors for the ALD process.

Experimental Procedure—ALD Process: Fiji F200 from Cambridge Nanotech, equipped with a remote plasma generator, was used for the ALD deposition process. Argon gas flowed continuously through the machine at a 260 standard cubic cm per min (sccm) flow rate, and the chamber temperature was set to 80 °C. The throttle valve at the end of the chamber was partially closed to set the base pressure to ≈300 mTorr. During each ALD process, a single layer of fabric was inserted into the system. Before coating, a plasma generator (13.56 MHz) was activated for 1 min at 300 W, with oxygen flow of 30 sccm and argon flow of 200 sccm, in order to increase the UHMWPE fibers' surface reactivity. Each ALD cycle consisted of a 0.06 s pulse of trimethylaluminum (TMA), followed by a 30 s purge, and a 0.06 s pulse of water, followed by a 60 s purge. The alumina coating thickness measurement was done using a Nanofilm_ep4 Ellipsometer from Accurion. A 32 ± 3 nm thick alumina layer was deposited after 350 cycles, as measured by ellipsometry on a silicon wafer that was present in the chamber during the deposition process. This value represents an alumina growth rate of 0.8–1.0 Å $cycle^{-1}$ on the silicon wafer. Previous works measured an accelerated alumina growth rate of 2.6 Å $cycle^{-1}$ on polyethylene during the first 40 ALD cycles. After this initial stage, a conformal alumina ALD film is formed, and the growth rate on the polymer surface is similar to the growth rate on the silicon wafer. Due to this accelerated growth rate,[31,58,59] the actual thickness of the alumina layer on the UHMWPE fibers was estimated at 39 ± 4 nm. Additionally, in order to verify the ALD coating stability, its characterization and the composite lamination

process were performed three weeks after completion of the ALD process.

Experimental Procedure—Laminate Fabrication: Composite laminates were prepared by symmetric 0°/90° wet hand-layup of five layers of UHMWPE fabric. Each layer was settled in place by a paint brush dipped in the epoxy adhesive, already mixed at 100:38 w/w parts of resin:hardener, according to the manufacturer's recommendations.[60] Each layer was plastered into place by a metal roller. The laminate was then covered with three sets of additional process fabrics—breather, perforated paper, and absorber paper—to absorb the excess resin, and then a vacuum bag. The curing process was initiated after a mobile vacuum inducer was connected. Excess resin was evacuated during the first stage of curing at room temperature (RT) for 24 h. A second stage of curing was followed for 15 h at 50 °C. Specimens were cut by a jigsaw with a 0.5 mm thick blade. The specimens were abraded around their edges to a final dimension of 20 mm × 10 mm × 2 mm, first on a 400-grit paper, then on a 600-grit paper.

Characterization Techniques: The surface morphology of UHMWPE fibers was analyzed using a multimode Nanoscope IV atomic force microscope (AFM) from Veeco in an intermittent contact mode. The measurement was performed using a silicon tip. The scans were performed at a drive frequency of 80 kHz and a drive amplitude of 1 V. Images were analyzed with Gwyddion software. The image processing method is described in Section 2 of the Supporting Information.

Water droplets contact angle on the UHMWPE fibers were measured at micron-scale in Quanta 200 field-emission gun ESEM. Images were obtained using a secondary electrons (SE) detector at a working distance of 4 mm. At the beginning of the experiment, the Peltier stage, which held the sample, was stabilized at 2 °C while the vapor pressure in the chamber was held at 5.3 Torr. By increasing the chamber pressure above dew point, vapor water condensation produced water droplets on the UHMWPE fiber surface, which were analyzed for contact angle size.[61,62] The contact angles were measured by Gwyddion software. The average of 30 measurements for each population was calculated.

A section of the fabric was cut and was spread on the sample holder in order to verify the alumina layer formation on the fabric. Using 20 kV acceleration voltage, an Oxford X-MAX EDS detector was used to identify the alumina layer formation in the upper as well as the lower layers of fibers within the UHMWPE fabric.

HRSEM images of the surface of UHMWPE-epoxy composites were acquired at a low acceleration voltage of 1 keV, using a Sigma 300 VP microscope from Zeiss. Images were obtained from the SE detector at a working distance of 4 mm. DMA was performed using a DMA Q800 from TA. This machine was used for mechanical properties evaluation of single fibers as well as composite samples. Evaluation of the alumina coating effect on the mechanical properties of UHMWPE single fibers was performed by wrapping the fibers around a C-shaped aluminum foil and gluing the fibers to the upper and lower ends of the foil, using a cyanoacrylate glue. The C-shaped aluminum foil was attached to the DMA tension clamps, and its center part was cut before measuring. The samples were stretched at a rate of 1 N min^{-1} at RT. Prior to each test, the sample's diameter was measured using an optical microscope; each test was repeated ten times. The force was normalized by the fiber's circular cross-section, which was verified by fractographic characterization.[63] A frequency sweep test was conducted at 35 °C, with a preload force of 0.1 N, oscillatory strain of 0.15%, and a frequency sweep spanning from 0.05 Hz to 200 Hz. Each test was performed five times.

Mechanical properties were also tested on a Lloyd tensiometer equipped with a 5 kN load cell. Three-point bending setup was used for stress–strain measurements, with a span-to-specimen thickness ratio of 5 as recommended by ASTM D 2344.[64–68] Each population was tested 15 times. The deflection rate was set to 1 mm min^{-1}, with an initial force of 1 N, at RT. All samples were conditioned at RT for 24 h prior to testing. Student's *t*-test was carried out to determine the level of statistical significance of the results ($p < 0.01$).

Supporting Information

Supporting Information is available from the Wiley Online Library or from the author.

Acknowledgements

The authors would like to thank Dr. Yacov Carmiel and Ms. Meital Ozeri for their support in this work. The authors would also like to thank the Israeli Department of Defense for its funding (Grant No. 4440830885).

Conflict of Interest

The authors declare no conflict of interest.

Keywords

composite materials, functional coatings, surface modification, thin films, UHMWPE

Received: February 22, 2018
Revised: April 18, 2018
Published online:

[1] P. Smith, P. J. Lemstra, *Polymer* **1980**, *21*, 1341.
[2] T. Kanamoto, A. Tsuruta, K. Tanaka, M. Takeda, R. S. Porter, *Polym. J.* **1983**, *15*, 327.
[3] M. R. Anton, C. Mackley, *Polym. Bull.* **1987**, *29*, 175.
[4] K. P. Menard, *Dynamic Mechanical Analysis: A Practical Introduction*, 2nd ed., CRC Press, London **2008**.
[5] Y. Termonia, P. Smith, *Macromolecules* **1987**, *20*, 835.
[6] L. Berger, H. Kausch, C. J. Plummer, *Polymer* **2003**, *44*, 5877.
[7] H. Harel, G. Marom, S. Kenig, *Appl. Compos. Mater.* **2002**, *9*, 33.
[8] I. Meshi, I. Amarilio, D. Benes, R. Haj-ali, *Composites, Part B* **2016**, *98*, 166.
[9] M. J. N. Jacobs, Technische Universiteit Eindhoven, **1999**.
[10] M. Deng, R. A. Latour, A. A. Ogale, S. W. Shalaby, *J. Biomed. Mater. Res.* **1998**, *40*, 214.
[11] M. S. Silverstein, O. Breuer, *J. Mater. Sci.* **1993**, *28*, 4718.
[12] M. Ahmadi, M. Masoomi, S. Safi, O. Zabihi, *J. Appl. Polym. Sci.* **2016**, *133*, 1.
[13] H. Liu, Y. Pei, D. Xie, X. Deng, Y. X. Leng, Y. Jin, N. Huang, *Appl. Surf. Sci.* **2010**, *256*, 3941.
[14] Y. F. Fu, K. Xu, J. Li, Z. Y. Sun, F. Q. Zhang, D. M. Chen, *Polym. Plast. Technol. Eng.* **2012**, *51*, 273.
[15] E. H. Cho, S. G. Lee, J. K. Kim, *Curr. Appl. Phys.* **2005**, *5*, 475.
[16] X. Zhang, Y. Wang, C. Lu, S. Cheng, *Polym. Bull.* **2011**, *67*, 527.
[17] N. H. Ladizesky, I. M. Ward, *J. Mater. Sci.* **1989**, *24*, 3763.
[18] A. Zhamu, M. Wingert, S. Jana, *Composites, Part A* **2007**, *38*, 699.
[19] Z. Z. W. H. Shi, *Compos. Interfaces* **2017**, *15*, 35.
[20] D. C. Davis, J. W. Wilkerson, J. Zhu, V. G. Hadjiev, *Compos. Sci. Technol.* **2011**, *71*, 1089.
[21] X. Jin, W. Wang, L. Bian, C. Xiao, G. Zheng, C. Zhou, *Synth. Met.* **2011**, *161*, 984.
[22] H.-T. Chiu, J.-H. Wang, *J. Appl. Polym. Sci.* **1998**, *68*, 1387.
[23] J. Maity, C. Jacob, C. K. Das, S. Alam, R. P. Singh, *Polym. Test.* **2008**, *27*, 581.
[24] J. Wang, G. Liang, W. Zhao, S. Lü, Z. Zhang, *Appl. Surf. Sci.* **2006**, *253*, 668.

[25] Y. Zhang, J. Yu, L. Chen, J. Zhu, Z. Hu, *J. Macromol*, *Sci. Part B* **2009**, *48*, 391.
[26] Y. Zhang, J. Yu, C. Zhou, L. Chen, Z. Hu, *Polym. Compos.* **2009**, 684.
[27] L. R. Vargas-Gonzalez, S. M. Walsh, D. D. Pappas, *Polym. Compos.* **2012**, *33*, 207.
[28] H. Liu, D. Xie, L. Qian, X. Deng, Y. X. Leng, N. Huang, *Surf. Coat. Technol.* **2011**, *205*, 2697.
[29] C.-Y. Huang, J.-Y. Wu, C.-S. Tsai, K.-H. Hsieh, J.-T. Yeh, K.-N. Chen, *Surf. Coat. Technol.* **2013**, *231*, 507.
[30] S. M. George, *Chem. Rev.* **2010**, *110*, 111.
[31] J. D. Ferguson, A. W. Weimer, S. M. George, *Chem. Mater.* **2004**, *16*, 5602.
[32] M. Kemell, E. Färm, M. Ritala, M. Leskelä, *Eur. Polym. J.* **2008**, *44*, 3564.
[33] S. Katz, Y. Carmiel, I. Gouzman, C. Sukenik, H. D. Wagner, E. Grossman, *MRS Proc.* **2013**, *1499*.
[34] Z. Li, W. Zhang, X. Wang, Y. Mai, Y. Zhang, *Appl. Surf. Sci.* **2011**, *257*, 7600.
[35] S. Jana, G. Sui, W. H. Zhong, *J. Adhes. Sci. Technol.* **2009**, *23*, 1281.
[36] R. Intrater, A. Hoffman, G. Lempert, I. Gouzman, E. Grossman, *Polym. Degrad. Stab.* **2006**, *91*, 1948.
[37] T. Jõgiaas, T. Arroval, L. Kollo, J. Kozlova, T. Käämbre, H. Mändar, A. Tamm, I. Hussainova, K. Kukli, *Phys. Status Solidi* **2014**, *211*, 403.
[38] Q. Peng, B. Gong, G. N. Parsons, *Nanotechnology* **2011**, *22*, 155601.
[39] A. K. Roy, W. Baumann, I. König, G. Baumann, S. Schulze, M. Hietschold, T. Mäder, D. J. Nestler, B. Wielage, W. a. Goedel, *Anal. Bioanal. Chem.* **2010**, *396*, 1913.
[40] S. D. Elliott, G. Scarel, C. Wiemer, M. Fanciulli, G. Pavia, *Chem. Mater.* **2006**, *18*, 3764.
[41] Z. Barkay, G. Roy, Y. Gabay, B. Yehuda, *J. Chem. Chem. Eng.* **2016**, *1*, 42.
[42] C. Ton-That, A. G. Shard, D. O. H. Teare, R. H. Bradley, *Polymer* **2001**, *42*, 1121.
[43] M. Brugnara, *Microscopy and Analysis* **2007**, *21*, 17.
[44] Z. Barkay, *Langmuir* **2010**, *26*, 18581.
[45] C. H. Cheng, H. H. Lin, *IEEE Trans. Adv. Packag.* **2008**, *31*, 100.
[46] J. George, M. S. Sreekala, S. Thomas, *Polym. Eng. Sci.* **2001**, *41*, 1471.
[47] A. Bhattacharyya, *eXPRESS Polym. Lett.* **2013**, *8*, 74.
[48] M. Ahmadi, O. Zabihi, M. Masoomi, M. Naebe, *Compos. Sci. Technol.* **2016**, *134*, 1.
[49] W. Li, L. Meng, L. Wang, J. Mu, Q. Pan, *Surf. Interface Anal.* **2016**, *48*, 1316.
[50] L. T. Drzal, M. Madhukar, *J. Mater. Sci.* **1993**, *28*, 569.
[51] M. S. Madhukar, L. T. Drzal, *J. Compos. Mater.* **1991**, *25*, 932.
[52] K. P. Menard, *Dynamic Mechanical Analysis: A Practical Introduction*, CRC Press, London **1999**.
[53] A. Levi-Sasson, I. Meshi, S. Mustacchi, I. Amarilio, D. Benes, V. Favorsky, R. Eliasy, J. Aboudi, R. Haj-Ali, *Composites, Part B* **2014**, *57*, 96.
[54] X. Zhuang, X. Yan, *Compos. Sci. Technol.* **2006**, *66*, 444.
[55] P. J. Kinlen, V. Menon, Y. Ding, *J. Electrochem. Soc.* **1999**, *146*, 3690.
[56] E. Vaca-cortés, M. A. Lorenzo, J. O. Jirsa, H. G. Wheat, R. L. Carrasquillo, *Adhesion Testing of Epoxy Coating (Report No. 1265-6)*, Texas **1998**.
[57] E. C. Botelho, R. A. Silva, L. C. Pardini, M. C. Rezende, *J. Adhes. Sci. Technol.* **2004**, *18*, 1799.
[58] C. A. Wilson, R. K. Grubbs, S. M. George, *Chem. Mater.* **2005**, *17*, 5625.
[59] M. D. Groner, F. H. Fabreguette, J. W. Elam, S. M. George, *Chem. Mater.* **2004**, *16*, 639.
[60] Huntsman, *Araldite ® LY 5052/Aradur ® 5052*, **2007**.
[61] Z. Barkay, *Microsc. Microanal.* **2012**, *18* (Suppl. 2), 1134.
[62] Z. Barkay, *Imaging Microsc.* **2013**, *15*, 51.
[63] M. Shimel, *M.Sc. Thesis*, Tel-Aviv University, **2017**.
[64] M. R. Wisnom, T. Reynolds, N. Gwilliam, *Compos. Sci. Technol.* **1996**, *56*, 93.
[65] L. V. da Silva, J. H. S. a. Junior, C. C. Angrizani, S. C. Amico, *J. Reinf. Plast. Compos.* **2012**, *32*, 197.
[66] Z. Fan, M. H. Santare, S. G. Advani, *Composites, Part* **2008**, *39*, 540.
[67] M. P. Kumar, V. B. Murthy, *Int. J. Eng. Res. Technol.* **2012**, *1*, 1.
[68] A. P. Mouritz, J. Gallagher, A. A. Goodwin, *Compos. Sci. Technol.* **1997**, *57*, 509.

